

# **Denoising Convolutional Neural Network with Energy-Based Attention for Image Enhancement**

Karthikeyan V<sup>1</sup>, Raja E<sup>2</sup>, Gurumoorthy G<sup>3</sup>

1-AP/ECE, Mepco Schlenk Engineering College, Sivakasi, Tamilnadu, India

2-AP/ECE, SRM-TRP Engineering College, Trichy, Tamilnadu, India

3- AP/EEE, PSR Engineering College, Sivakasi, Tamilnadu, India

## **ABSTRACT**

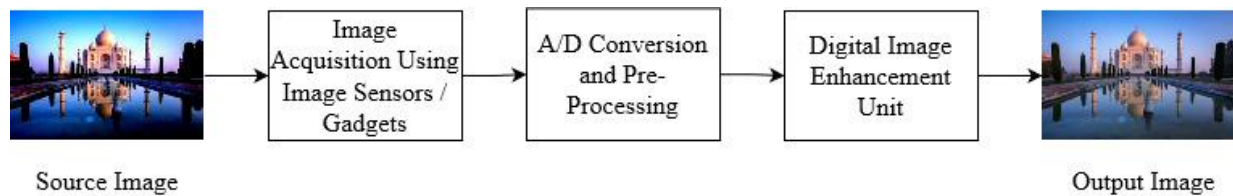
In the realm of image denoising, the use of convolutional neural networks (CNNs) has lately gained traction. Several activities involve the utilization of excellent-clarity pictures and recordings. Images were captured in a wide variety of illumination circumstances, which means that not all of them are of the highest quality. Low-light photography suffers from a decline in perceived image quality because of the restricted dynamic range of the pixel values. Therefore, it is vital to enhance the appearance of images. Maximum texture retention is achieved by the structural similarity index-loss-based method. The suggested discrete wavelet transform (DWT)-self attention (SA)-Denoising convolutional neural networks (DnCNNs) make use of state-of-the-art techniques for image denoising like energy band analysis, very deep architecture, learning algorithms, dense-sparse-dense training, and regularization approaches. DnCNN is intended to remove the hidden layers' latent, yielding a pure picture. After a degraded input sample has had its relevant energy features retrieved using DWT, the perfect image enhancement is achieved thanks to the incorporation of the self-attention mechanism. Second, a hierarchical-branch network is formed by combining the suggested network with the denoising CNN and additional loss in order to reduce the reliance on the amount of noisy data in multi-modal picture analysis and make the problem of image enhancement more tractable. In the end, DWT-SA-DnCNN's self-learning qualities are used to improve image quality by obtaining features including undesirable noisy data, edge factor, texture, uniform and non-uniform areas, smoothness, and object structure. Simulation results show that our hybrid DWT-SA-DnCNN-based contrast enhancement strategy outperforms state-of-the-art methods.

**Keywords:** Image Enhancement, Self-Attention, SSIM, CNN, DWT, PSNR

## **1. INTRODUCTION**

Image processing, also referred to as IP, encompasses the conversion of an image to a digital format, followed by the execution of diverse operations with the purpose of enhancing the image or extracting pertinent data. In addition, it constitutes a substantial area of research

within the disciplines of computer science and engineering. Using a variety of image acquisition technologies to import images into the computer constitutes the initial stage in the image processing workflow. Subsequently, processes including image analysis, retouching, and analysis are performed to generate the final product, which consists of modified photographs. Analogue image processing and digital picture processing are two distinct types of image processing. It is feasible to improve physical duplicates, including photographs and prints, by employing analog image processing techniques. Image analysts utilize an extensive range of interpretive principles in their interactions with these visual instruments. The illustration in Figure 1 illustrates how "digital image processing" pertains to the modification of digital photographs via personal computers.



**Figure 1. Image Enhancement**

The proliferation of cameras on a wide variety of consumer electronics devices has resulted in a meteoric rise in the amount of image content being produced. The bulk of the time, significant form deterioration occurs during the process of image capture. It could be attributed to the physical constraints of the camera's lens, or it could be owing to the lighting conditions. Due to the small size of the sensors in smartphones, for instance, the aperture is extremely narrow, and the depth of field is severely restricted. As a direct consequence of this, their photographs are typically grainy and lack contrast. Poor lighting results in photographs that are generally too black or overly brilliant, depending on the circumstances. The goal of the image recovery competition is to find a way to reconstruct a high-quality version of an image using just its impaired characteristics. This is a poorly stated inverse problem since there are numerous different outcomes that could occur (Alisha and Gnana Sheela, 2016; Fan *et al.* 2019; Kaur *et al.* 2018; Liu *et al.* 2018).

Within the realm of computer vision, the concept of image enhancement is one that is both ubiquitous and fundamental. A few images have low resolution caused by external influences, including the environment and illumination, that may impact the efficacy of applications that use computer vision, like automated public transport, image cognitive ability, and consumer

products. Despite the fact that digital technology has made significant improvements in efficiency, some pictures have a poor standard due to these external factors (Han *et al.* 2018). Particularly difficult to see are photographs with low contrast. As a consequence of this, numerous high-tech devices now assist users in acquiring photographs and enhancing the quality of those photographs through the incorporation of inbuilt imaging techniques. These devices do, however, require a few parameters from the individual using them, including the selection of an area that has minimal brightness or a typical luminance and hue (Li *et al.* 2015). Under specific conditions, it is an ideal choice for equipment users who do not prioritize image visibility, such as purposely capturing contrary light images. However, simple equipment users would consider it inappropriate to solely adjust the hue tone and increase the overall luminance when attempting to restore a visual. Enhancing the low-intensity portion of the original photos while maintaining image clarity is a difficult undertaking (Jain *et al.* 2007).

Many quantitative learning techniques and traditional IP methodologies have been proposed as potential solutions to this issue under certain conditions; however, these solutions either fail in other contexts or have unintended consequences, including the halo effect or over-enhancement (Portilla *et al.* 2003). To mitigate the drawback, several enhancement strategies employ optimization strategies coupled with an image decomposition methodology. The reconstruction duration increases, and unanticipated adverse consequences are possible if we depend on the intended details with decomposed components. These disadvantages make the techniques less than optimal for the use of simpler equipment (Kim *et al.* 2016).

The clarity and accuracy of damaged photographs can be improved with the help of image enhancement (IE) techniques. In the realm of image rehabilitation, CNNs like low-light CNN and super-resolution CNN have proven very effective (Hu *et al.* 2021). In this research, DWT, an attention technique, and a denoising CNN are all integrated to produce IE. The two parameters used to compare various methods of picture restoration are the peak signal-to-noise ratio (PSNR) and the structural similarity index (SSIM). When compared to alternative approaches, the presented approach has superior PSNR and SSIM statistics.

In summary, our main contributions are the following:

- ♦ An innovative energy-based attention network with a denoising convolutional neural network (EBAN-DnCNN) is proposed for improving image quality. EBAN improves the visibility of

the image, apart from improving the image itself. We attain state-of-the-art status by simplifying the low-level IE issue this way.

◊ Developed a supervised attention technique for training a DnCNN model based on energy maps. Video processing issues in different lighting circumstances is solved by combining an energy-based self-attention module with a deep denoising convolutional neural network. This combination can bypass the need for raw camera file images and complete tasks using a common image file.

◊ Significant improvements in performance have been achieved in several datasets, encompassing both real and artificially generated low-level lighted images.

The remainder of the paper is structured as follows: Image contrast enhancement is discussed in depth in Section 1. Image dehazing-related works are collected in Section 2. In Section 3, we discuss how the suggested hybrid DWT-SA-DnCNN approach can be used to restore images. In Section 4, we present the results of an experimental examination of picture denoising using the suggested approach. In the final section of the study, we evaluate the prospects of this topic.

## 2. RELATED WORKS

Surveillance, photographic imaging, radiation therapy, and satellite imagery all make use of image augmentation. For position-sensitive image restoration, exact pixel-by-pixel compatibility between the original and restored images is required. This is why it's so important to just discard corrupted image data while preserving spatial properties like texture and edges. Until recently, artificial neural network systems struggled due to a lack of data and processing power. The proliferation of both computing resources and information has made artificial neural networks useful for numerous contexts ([Karthikeyan et al. 2023](#)). Advantages based on the input image parameters have been found when more learning approaches are investigated.

Image enhancement (IE) is employed to improve the visual quality of images and boost the knowledge available for further assessment and process ([Liu et al. 2017](#); [Zollini et al. 2020](#); [Dominici et al. 2019](#)). Various poor lighting image improvement methods have been proposed and have achieved significant advancements in the fields of image augmentation and remotely acquired images. Histogram Equalization (HE) and its variations, such as Dynamic Histogram Equalization, Brightness Protecting Dynamic Histogram Equalization, and Contrast Constrained Adaptive Histogram Equalization (CLAHE), are conventional methods for

enhancing contradiction in images. These strategies have been studied and discussed by various researchers, including [Gonzalez \*et al.\* \(2009\)](#), [Abdullah-Al-Wadud \*et al.\* \(2007\)](#), [Ibrahim & Kong \(2007\)](#), [Asha & Sreenivasulu \(2018\)](#), and [Pisano \*et al.\* \(1998\)](#). Additionally, contrast improvement in low-light images can be achieved through histogram equalization and illumination adjustment ([Banik \*et al.\* 2018](#)). Other approaches, such as the Retinex-based theory ([Lank, 1977](#)) and the multiscale Retinex model (MSR-net) ([Jobson \*et al.\* 1977](#)), are also utilized for contrast restoration. The objective of high dynamic range is to enhance the relative quality of an image by expanding its dynamic span. This is a worldwide alteration that disregards variations in brightness, leading to specific areas being excessively exposed, causing deformation in hue, and inadequate suppression of noise. This method may generate photos with increased luminosity and contrast without any manual involvement. Nevertheless, the highlighting of features in low-light regions is inadequate, and there is a possibility of color aberrations ([Wang \*et al.\* 2004](#); [Tao \*et al.\* 2017](#)). Deep learning (DL) presents a revolutionary low-light IE approach [Guo \*et al.\* \(2017\)](#). Low-light performance can be improved using a variety of DL-based techniques, including brightness assessment and explicit training throughout the process which is summarized in Table 1.

**Table 1.** Deep Learning-Based Methods for IE

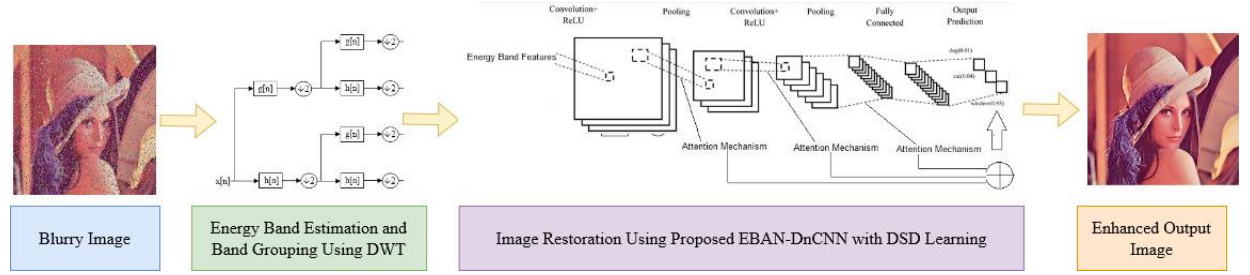
Reference	Inference
<a href="#">Fu <i>et al.</i> (2015)</a>	Suggested a stochastic image deconstruction. After partitioning the source image into brightness and backscattering scenarios, the optimum post-processing technique estimated enhanced brightness and contemplation.
<a href="#">Ying <i>et al.</i> (2017)</a>	The camera response model improved low-light images. Camera responsiveness and illumination transformation are CRM subcategories. These methods and an estimated illumination proportion map improve low-light pixels.
<a href="#">Li <i>et al.</i> (2018)</a>	Proposed a convolutional neural network for improving low-light images. LightenNet consists of four distinct stages. After a four-convolutional-layer network has estimated the lighting conditions, the brightness map is improved using gamma compensation and a directed image filter
<a href="#">(Lore <i>et al.</i> 2017)</a>	The end-to-end approach stacked sparse denoising autoencoder developed on synthetic information can enhance and denoise low-light images with noise-sensitive emphasis, Low-light Net (LLNet) creatively expands ( <a href="#">Xie <i>et al.</i> 2012</a> ).
<a href="#">Ai &amp; Kwon (2020)</a>	Suggested Attention U-net convolutional network, works well in very dim conditions and does not require raw image files to solve the problem of smart city video surveillance security.

Traditional and AI approaches to the analysis of remotely sensed low-light photos continue to dominate the field. There have been a number of attempts to enhance low-visibility aerial images; for example, [Fu et al. \(2015\)](#) used HE to increase contrast, [Lee et al. \(2012\)](#) employed dictated irradiation and dynamic brightness adjustment, [Li et al. \(2018\)](#) offered multifaceted wavelet transform approaches, and [Liu et al. \(2017\)](#) used Retinex analysis. Despite premiering in the late 1970s, the 2000s were CNN's most successful era. [Jung and Oh demonstrated in 2004](#) that GPUs could construct neural networks at a 50% faster rate than CPUs. Today, deep learning is not given the respect it deserves. A study by [Singh and Shree in 2020](#) and by [Lee et al. in 2015](#) found that convolutional networks perform exceptionally well in low-light image processing. Most neural networks have extensive training. Training generates random NN weights. Using the dense-sparse-dense (DSD) technique, [Han et al. \(2016\)](#) achieved superior outcomes when training GoogLeNet, VGG-16, ResNet-16, Deep Speech, and other networks. The following image enhancement techniques used DL: super-resolution ([Kim et al. 2016](#)), MSR-net ([Shen et al. 2017](#)), GLADNet ([Wang et al. 2018](#)), and poor-light IE by Illumination Map Estimation (LIME) ([Guo et al. 2016](#)). LIME exhibits exceptional efficacy in scenarios involving images with little or no lighting, wherein the author devises a sophisticated averaging framework to accurately compute the illumination map.

When compared to more traditional methods of picture restoration, the proposed DWT-SA-denoising CNNs perform exceptionally well. The quantity of energy in each sub-band was calculated using the discrete wavelet transform so that the most suitable frequency range could be selected. The convolutional neural network with the SA-based denoising technique uses many kernels to collect features as varied as textures, borders, contours, and bottleneck features associated with energy sub-bands. Next, the combination of feature mappings is used to generate the final, improved visuals. In addition, the denoising CNN framework for IE is trained employing synthetic low-light and normal-light image sets utilizing dense sparse dense training in this study. This article's strong augmentation effectiveness can be attributed to its few parameters, low computing resource consumption, and lack of particular heterogeneity. All the methods shown here, which are based on a mix of DWT and SA-DnCNN, can be used with both high-resolution and lower-resolution interpretations. Therefore, an instantaneous multi-class IE strategy can benefit from the use of a convolutional neural network trained on projected energy to remove noise.

### 3. MATERIALS AND METHODS

This part will initially explore the energy estimation and spectrum aggregation techniques relying on the wavelet transform. After that, the chunk information is put into a DnCNN model that uses self-attention and has fewer layers and a dense sparse dense learning architecture. Ultimately, the process of image restoration is executed in accordance with the depiction shown in figure 2.



**Figure 2. Block diagram of Suggested system**

#### 3.1. Estimating energy bands using Discrete Wavelet Transform

Assessment of energy systems centers on the principle of conserving energy. Estimate the energy % by calculating the detailed coefficients (D) as well as the approximated coefficients (A). In the wavelet-based realm, Parseval's principle reflects the principle of conservation of energy. The discrete wavelet transform's basic consuming power is equal to the square summation of each band's harmonic constituents. The acquired image  $J$  is inputted into the DWT processing module.

$$\frac{1}{N} \sum_v |J(v)|^2 = \frac{1}{N_L} \sum_m |A_{l,m}|^2 + \sum_{l=1}^L \left\{ \frac{1}{N_L} \sum_m |D_{l,m}|^2 \right\} \quad (1)$$

Band energy can be calculated by evaluating specific and quantitative characteristics, which provide the foundation for energy assessment that utilizes intelligent band selection (1). The target spectrum was split up into several, equally-sized subbands utilizing a finite impulse response filter. Using DWT, we analyzed the obtained blurry images and determined the percentage of energy in each band of frequencies (Ma et al., 2020). First, the work herein employed DB1 wavelets to calculate the detailed and analysis components' energy levels. The percentage of the band's energy that is contained in its subbands can be calculated after



applying DWT tenfold (with L equal to 1). The following procedure for calculating percentages is derived from doing energy normalization on the band:

$$S_{E_q} = \frac{\frac{1}{N_L} \sum_m |A_{L,m}|^2}{\frac{1}{N} \sum_v |J(v)|^2} \quad \text{or} \quad \frac{\frac{1}{N_L} \sum_m |D_{L,m}|^2}{\frac{1}{N} \sum_v |J(v)|^2} \quad (2)$$

Here  $S_{E_q}$  represents the sub-band energy percent, and  $L=1$ .

### 3.2. Improved DnCNN with attention mechanism

#### 3.2.1. Attention-based modules

The attention process in deep learning is similar to the visual attention of humans, where it focuses on material that is most relevant to the final result. In order to enhance the efficiency of the image enhancement process, we incorporated an attention strategy into the DnCNN model. Figure 3 illustrates the implementation of the suggested approach. The local energy characteristic refers to the provisional outcome of the DnCNN framework, and it is denoted by blocks 1/2/3. The convolutional and regressive layers in the network utilize all elements of the source image as parameters, and Block 4 is a comprehensive energy characteristic that produces outputs. The attention strategy received knowledge on energy qualities at both local and global levels, and the estimator has the ability to generate new feature maps to replace the image's specific features (Ai & Kwon, 2020). Finally, the result is obtained at an inverse discrete wavelet transform (IDWT) block, which is subsequently proceeded by a fully connected layer (FC-2, 1024). The procedure commences by combining the outcomes of many local feature maps with the final layer of the DnCNN. The layout of the attention estimator, which is task-driven, is illustrated in Figure 4. A  $1 \times 1$ -convolution kernel is employed to limit the dimensionality of the local data to one, followed by the application of the softmax operator to normalize the results. The inputs consist of both the interim characteristics and the generic attributes. Subsequently, Block 4 is employed to normalize characteristics through element-wise scaling. We modify the conventional architecture to improve input images by utilizing a weighted blend of local and global characteristics. Additionally, we establish a compatibility metric between local and global features to ensure that the network is incentivized to learn attention patterns that are crucial for completing the given task.

#### 3.2.2. Hybrid DWT-SA-DnCNN architecture



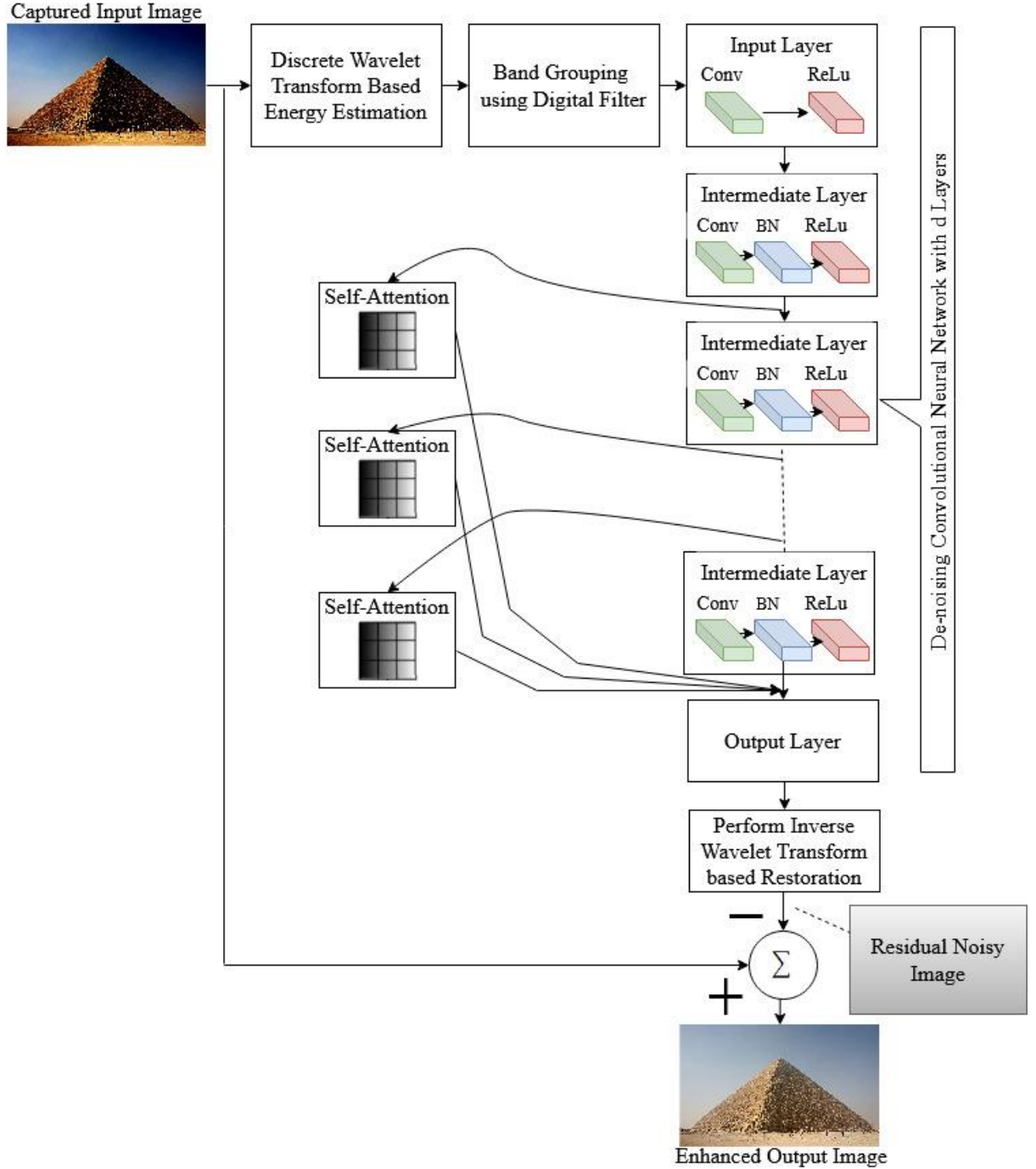
The suggested hybrid DWT-SA-DnCNN architecture for enhancing visual contrast is depicted in Figure 3. Attention-weighted energy band chunks are sent to the CNN that is de-noising for the purposes of persistent training and normalization. Convolution layers number  $d$  (10) in this network. Besides the output layer, a ReLU activates all the other layers. Batch normalization (Ioffe & Szegedy, 2015) is utilized across every subsequent convolution layer to prevent the inner correlation distortion generated by mounting several layers. Instead of learning a clear image, a residual pattern is picked up. The residual learning method (He et al., 2016) eliminates noise in the source images to boost accuracy. One advantage of the hybrid DnCNN is that SA-DWT has very low energy constraints.

The 'd' layer is present in the suggested composite DnCNN system. A deep CNN-based structure mines the energy bands of input images that are noise-filled in order to extract speculative qualities and accumulate particular traits. To avoid losing information due to color space conversion, a hybrid DWT-SA-DnCNN method could be used to assess multi-channel pictures. The complex nonlinear resemblance connections involving low-light and normal-light visual pairs can be trained to perfection, resulting in images with realistic lighting and contrast. Ignore all pooling layers and modify convolutional filters to  $3 \times 3$ . This means that for every given depth  $d$ , the reception field of DnCNN should be  $(2d+1)$ . Gaussian denoising with a custom noise variance can be achieved using DnCNN's  $21 \times 21$  receptive field% and 10 layer depth (Toshev & Szegedy, 2014). By increasing the depth to 13, the capabilities of picture denoising techniques are greatly enhanced.

DnCNN consists of three distinct kinds of layers. In Conv+ReLU, 64 feature maps are created with  $64 \ 3 \times 3 \times c$  filters in the first layer.  $C = 1$  for grayscale images, while  $c = 3$  for color ones. Conv+BN+ReLU:  $64 \ 3 \times 3 \times 64$  filters are used in Layers 2-D-1 for batch normalization among convolution and ReLU. In order to reconstruct the output, the last layer employs  $3 \times 3 \times 64 \ c$  filters.

Before applying convolution, a standard zero-padding approach is employed to smooth out irregularities at the borders. DnCNN uses convolution with a nonlinear activation function in the intermediate layers to distinguish visual from noise input. Inspired by the DSD training method, which trims down DnCNN model layers yet retains DWT (Han et al. 2016; Alawode et al. 2021). The suggested approach reduces DSD retraining and restorative times by focusing on learning at slower rates over lower energy bands. DSD is used to train energy-based DnCNNs

on energy band batches. Our key contribution is a method that preserves performance while decreasing the number of layers, parameters, and processing time required by DnCNN. We intend to simplify the design more (Alawode et al., 2021). The inverse DWT transform is used to obtain the remaining noisy image. The output is enhanced by subtracting the residual image from the original.



**Figure 3.** Proposed hybrid DWT-DnCNN Architecture

### 3.2.3. Loss function

The loss rate quantifies the disparity between predictions and ground truth, playing a vital role in system learning (Zhang *et al.* 2020). The model in this work was constructed using cross-entropy (CE), and structural similarity index (SSIM), and L2 loss functions. Equations (3) to (6) are used to compute network loss.

$$CE_l = - \sum_{p=0}^n x_p \log(\widehat{x}_p) \quad (3)$$

$$SSIM_l = \frac{(2\mu_a\mu_b + c_1)(2\sigma_{ab} + c_2)}{(\mu_a^2 + \mu_b^2 + c_1)(\sigma_a^2 + \sigma_b^2 + c_2)} \quad (4)$$

$$L2_l = \frac{1}{m} \sum_{p=0}^m (x_p - \widehat{x}_p)^2 \quad (5)$$

$$Loss\ function = CE_l + \alpha SSIM_l + (1 - \alpha) L2_l \quad (6)$$

Where  $CE_l$  is the loss of IE,  $L2_l$  is the loss of manual scored value regression.  $x_p$  and  $\widehat{x}_p$  denotes the predicted scores and manual scored value. In our network, a combine entropy, L2 loss and SSIM loss with a weight which usually appears in image enhancement methods. We set  $\alpha = 0.85$  in the learning process.

In order to discern between noise and incorrect input, this study creates an energy-wise attention-based DnCNN for image restoration, employing residual learning and DSD retraining. Training is expedited and restoration effectiveness is enhanced with reduced layer complexity by using energy-efficient techniques such as batch generation, DSD-training, BN, dropout, and residual training.



**Figure 4.** Proposed Hybrid DWT-DnCNN sample result

Figure 4 depicts the requirement for discrete models in conventional reconstruction approaches. Contrarily, this integrated energy-based attention paradigm is capable of stochastic Gaussian blurring with variable noise levels. In this study, we also demonstrated the capability of building a hybrid DnCNN strategy to execute visual deblocking with a set of recognized attributes, establish a high-resolution rendition of the image with different amenities, and modify the degree of noise in an image. Quantitative and qualitative image dehazing using the suggested method was demonstrated over a fair amount of time across multiple studies.

### 3.3. Dataset and Performance Metrics

In order to assess the efficacy of the proposed technique, this work employs both the industry-standard See-in-the-Dark (SID) dataset (Chen *et al.* 2018), SET14, SET 5 and real-time shots. The Sony 7SII and Fujifilm XT2 unprocessed sensor information included in the SID collection consists of 5094 short-exposure photos and 424 long-exposure images obtained in extremely dark environments.

After calculating conventional statistics to analyze the effects of several independent techniques, including the suggested approach, to assess image quality, the enhancement operation is performed to evaluate edge preservation and image structural metrics. This study employs these metrics: The structural similarity index (SSIM) compares the primary source image and the noise-removed output image. After processing, the peak signal to noise ratio (PSNR) measures denoised picture noise (Al-Najjar & Soong, 2012; Wang & Bovik, 2002). Equations (7)–(9) yield SSIM, PSNR, and MSE formulae. All of these formulas use  $X(k, l)$  to represent the pixels in the original noise-free image,  $N$  to represent the pixels in the degraded image, and  $R$  to represent the pixels in the output image after restoration.

$$SSIM(X, R) = \frac{(2\bar{x}\bar{r} + C_1)(2\sigma_{xr} + C_2)}{(\bar{x}^2 + \bar{r}^2 + C_1)(\sigma_x^2 + \sigma_r^2 + C_2)} \quad (7)$$

Here  $\sigma_x$  and  $\sigma_r$  indicates the standard deviations in the image  $X$  and  $R$ , and  $\sigma_{xr}$  specifies the standard deviation among the images  $X$  &  $R$ , and  $C_1$  &  $C_2$  are independent parameters that rely on the dynamic range ( $Z$ ), which are commonly set as  $C_1=0.01Z$  and  $C_2=0.03Z$ , respectively. The developers of SSIM assessments recommend using the default utilities of 0.01 and 0.03 to standardize the fraction's values and avoid a '0' in the divisor. The PSNR can be represented as:

$$PSNR = 10 \log_{10} \left( \frac{MAX_x^2}{MSE} \right) \quad (8)$$

and

$$MSE = \frac{1}{lm} \sum_{j=0}^{l-1} \sum_{k=0}^{m-1} [X(j, k) - N(j, k)]^2 \quad (9)$$

The mean square error is MSE, while  $MAX_x$  is the image X's greatest possible intensity value.

#### 4. RESULTS AND DISCUSSION

This subsection describes the experimental setting and the execution of the suggested DWT-SA-DnCNN performance for many different inputs. The recommended restorative method was then compared to contemporary techniques.

##### 4.1. Training and Testing

In all of the studies, PSNR, MSE, and SSIM were employed as benchmarks (Wang & Bovik, 2002; Al-Najjar & Soong, 2012). The models were created using the Python NN Keras toolbox, which relies on TensorFlow. Zhang et al. (2017) provide the DnCNN foundational model and training data. We used a Linux system with 32 GB of RAM and dual Nvidia GTX 1080 Ti GPUs for training and validating our models. To mimic the DnCNN's training method, we gave our DWT-SA-DnCNN a 40-epoch retraining epoch. The rate of learning and additional variables were kept constant, just like the traditional denoising CNN.

The efficacy of the proposed technique was assessed by subjecting it to various systems in Section 4.2. The presented approach was evaluated based on the constraints of noise variability. Every structure was trained utilizing hyper-parameters with kernel sizes that were identical to those recommended in the proposed methodology, for the sake of analysis. The proposed solution is notable because of the decoder's ability to rebuild. The without-skip and without-pooling stages produce the same outcomes. Pooling networks lack spatial information, while without-pooling layers possess a higher level of technical intricacy compared to without-skip layers. In their study, Shelhamer et al. (2017) demonstrated the efficacy of skip connections and pooling layers in employing precise annotated data. Training data-driven neural networks primarily provides predictions about test outcomes. This study demonstrated that the network structure and methodology had the potential to yield favorable outcomes, even in the presence of imprecise training data. Our DWT-SA-DnCNN achieved a training time similar to the regular DnCNN after 35 training epochs.

The DWT-SA-DnCNN's layering pattern and masking proportion are created during the training process, with fewer levels and a higher masking percentage than in the final architecture. Table 2 displays the complete findings. The outcomes indicate that the optimal compromise is ten layers with a masking efficiency of 12%. Network de-noising is not enhanced by trying more or fewer combinations. Approximately 86% of the weights in a dense network are effective in boosting performance, even with a masking rate of 14%.

**Table2.** Evaluation of the suggested method's efficiency across different layers and mask rates

Layer count	Assessment Metrics	% Weight Mask			
		8	10	12	15
8	PSNR	28.41	28.84	29.57	30.12
	SSIM	0.87	0.87	0.88	0.88
10	PSNR	30.98	31.28	32.98	32.51
	SSIM	0.89	0.91	0.94	0.93
12	PSNR	31.24	31.54	32.05	31.63
	SSIM	0.89	0.90	0.93	0.93
14	PSNR	31.18	32.27	32.25	32.06
	SSIM	0.91	0.92	0.94	0.93

#### 4.2. Qualitative Performance Assessment Outcomes

In order to evaluate the effectiveness of the recommended approach, this paper conducted a comparison with previous approaches like as CLAHE (Pisano *et al.* 1998), MSRCR (Rahman *et al.* 1996), Fu's method (Fu *et al.* 2015), Ying's method (Ying *et al.* 2017), attention-based structures (Zhang, C *et al.* 2020; Atoum *et al.* 2020), histogram equalization (HE) (Bassiou, & Kotropoulos, 2007), dynamic histogram equalization (DHE) (Abdullah-Al-Wadud *et al.* 2007), contrast growth of poor-light images using histogram equalization and illumination adjustment (Banik *et al.* 2018), the Retinex-based theory (Land, 1977), the multiscale Retinex model (MSR-net) (Jobson *et al.* 1997), LLNet suggested in (Lore *et al.* 2017), and DnCNN.



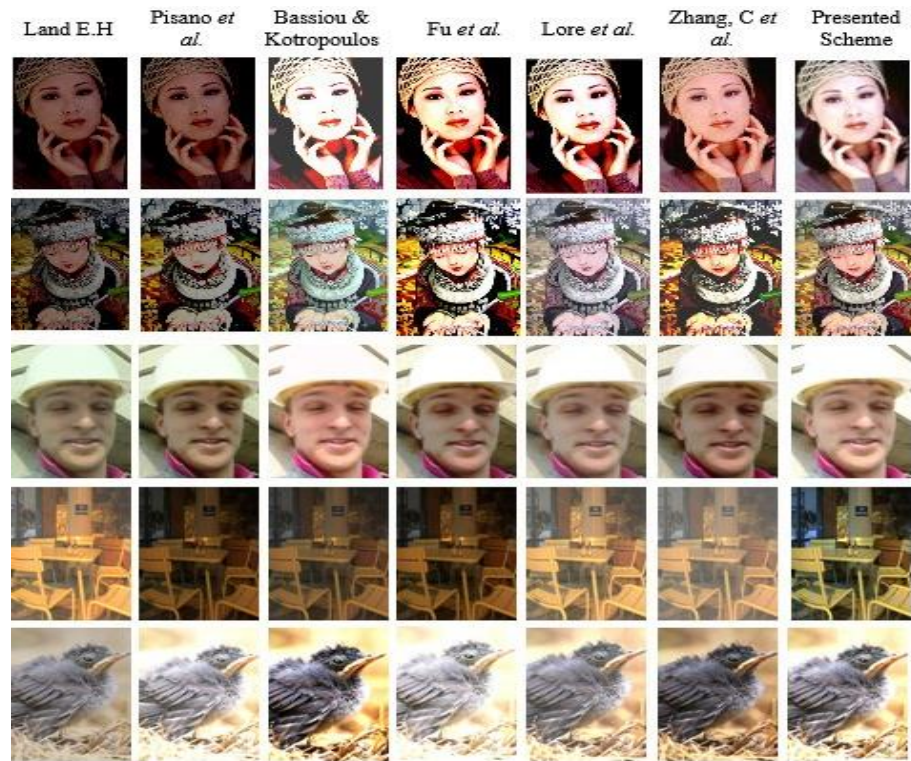


Figure 5 (a)

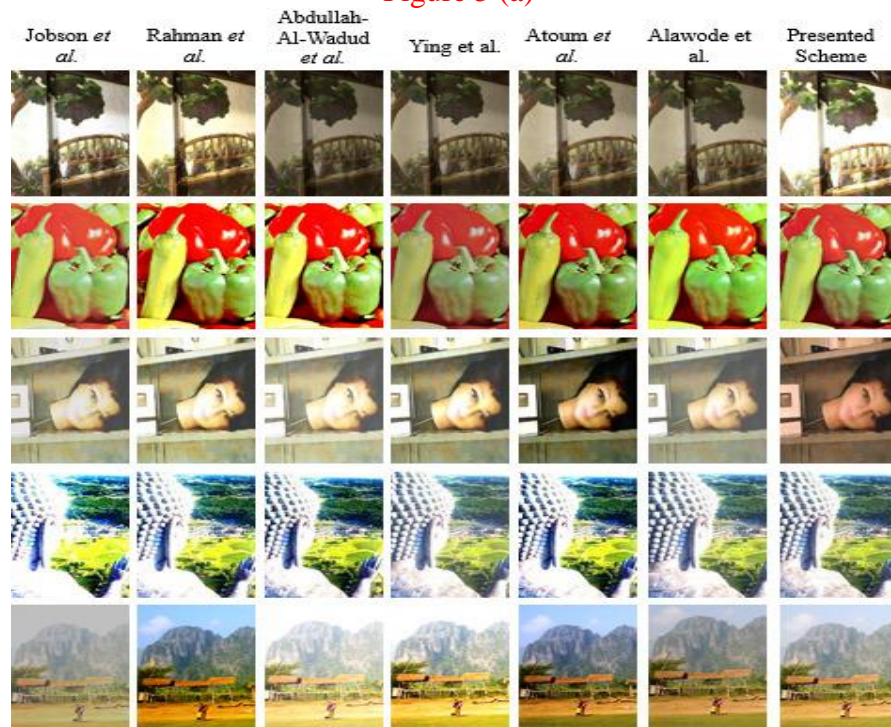


Figure 5 (b)

**Figure 5.** Qualitative performance of proposed strategy against traditional schemes

The outcomes of each restoration method are displayed in Figure 5. The first column of the original image in Figure 5 reveals dark and low-contrast exterior portions. The CLAHE, DHE,



and HE contrasts were nearly identical to the original pictures. Given that the source picture has both an input illumination and a dark section, the size and distribution of the subimage are governed by the spreading conditions. According to MSRCR and LLNet, the image appears and contrasts better than it does in CLAHE. Due to the intense sunlight, the sky always appears an identical color. The techniques used by Fu and Ying enhance both contrast and shape. But cumulative brilliance is inadequate. While DnCNN and attention-based methods outperform conventional contrast improvement techniques, they produce subpar illumination. Energy band batching and attention-based DSD retraining improve the traditional denoising CNN's performance, enabling it to automatically enhance image contrast while reducing the number of layers and difficulty. The performance of the proposed system is listed in Table 3.

**Table 3.** Evaluation of Different Restorative Methods in terms of PSNR (dB)/SSIM

Input	Restoration Methods							
	Fu <i>et al.</i> 2015	Banik <i>et al.</i> 2018	Zhang, C <i>et al.</i> 2020	Atoum <i>et al.</i> 2020	Lore <i>et al.</i> 2017	Ying <i>et al.</i> 2017	Denoising CNN	Suggested Scheme
<b>IMG 1</b>	33.56/ 0.84	40.56/ 0.87	41.74/ 0.96	42.36/ 0.95	36.25/ 0.86	37.31/ 0.89	39.72/ 0.95	<b>43.94/ 0.97</b>
<b>IMG 2</b>	35.32/ 0.85	40.02/ 0.91	40.56/ 0.93	41.98/ 0.92	37.58/ 0.88	39.24/ 0.90	39.58/ 0.91	<b>42.98/ 0.95</b>
<b>IMG 3</b>	34.27/ 0.84	39.64/ 0.88	40.92/ 0.92	41.54/ 0.93	38.14/ 0.89	38.45/ 0.88	38.87/ 0.89	<b>42.54/ 0.94</b>
<b>IMG 4</b>	17.55/ 0.79	22.45/ 0.80	26.62/ 0.87	24.90/ 0.83	20.63/ 0.79	22.47/ 0.81	25.36/ 0.84	<b>29.43/ 0.89</b>
<b>IMG 5</b>	20.04/ 0.60	21.10/ 0.64	24.90/ 0.83	25.36/ 0.86	21.96/ 0.77	22.16/ 0.84	26.42/ 0.86	<b>28.86/ 0.89</b>
<b>IMG 6</b>	14.85/ 0.25	21.33/ 0.78	24.21/ 0.79	23.11/ 0.79	20.00/ 0.60	24.54/ 0.79	20.98/ 0.74	<b>29.35/ 0.81</b>
<b>IMG 7</b>	22.33/ 0.78	22.47/ 0.81	25.38/ 0.87	26.82/ 0.89	25.32/ 0.85	24.36/ 0.86	23.75/ 0.82	<b>30.67/ 0.90</b>
<b>IMG 8</b>	20.00/ 0.60	21.55/ 0.70	25.15/ 0.76	26.42/ 0.79	24.76/ 0.74	23.19/ 0.73	25.71/ 0.78	<b>29.63/ 0.81</b>
<b>IMG 9</b>	19.98/ 0.62	25.48/ 0.83	28.47/ 0.88	29.23/ 0.90	28.15/ 0.87	27.59/ 0.86	27.60/ 0.87	<b>32.18/ 0.92</b>
<b>IMG 10</b>	24.25/ 0.80	26.54/ 0.85	29.76/ 0.86	31.15/ 0.88	28.55/ 0.87	29.64/ 0.88	30.53/ 0.89	<b>35.78/ 0.91</b>

#### 4.3. Qualitative Results with various noise conditions

Denoising images from articles were utilized to evaluate the systems. White Gaussian noise with certain variances was applied to original, unaltered images to generate the deteriorated

versions. Noise levels of 15, 20, 35, etc. were tested, as indicated in Table 4.

**Table 4. Quantitative Analysis of proposed Scheme against conventional schemes**







Test Sample Images	$\sigma$ Rate	Ying <i>et al.</i> 2017	Lore <i>et al.</i> 2017	Atoum et al. 2020	Zhang, et al. 2020	DnCNN	Proposed Method
	10	22.5/0.76	23.9/0.77	27.4/0.81	26.4/0.81	25.8/0.81	29.1/0.87
	20	21.7/0.68	20.8/0.68	21.6/0.74	22.2/0.76	21.1/0.74	27.6/0.79
	30	21.5/0.69	21.3/0.72	21.9/0.73	21.8/0.73	20.8/0.71	25.8/0.75
	40	22.3/0.70	22.1/0.71	24.7/0.74	25.1/0.79	24.6/0.73	28.2/0.82
	50	22.0/0.72	22.8/0.76	23.5/0.79	23.3/0.78	23.4/0.76	27.3/0.81
	10	24.4/0.72	26.7/0.75	27.3/0.78	28.4/0.81	25.6/0.74	32.2/0.86
	20	20.4/0.67	21.5/0.67	22.1/0.72	26.8/0.77	23.2/0.75	29.3/0.79
	30	18.5/0.62	19.7/0.64	21.2/0.66	22.7/0.71	20.5/0.67	23.8/0.75
	40	17.5/0.60	18.8/0.72	19.3/0.78	21.3/0.79	20.1/0.76	22.7/0.81
	50	16.4/0.59	18.2/0.70	19.2/0.73	20.1/0.76	17.9/0.65	22.3/0.80
	10	27.9/0.83	26.8/0.81	29.3/0.87	28.2/0.84	27.7/0.84	31.4/0.89
	20	26.5/0.81	26.2/0.80	27.7/0.83	27.3/0.81	27.0/0.81	31.1/0.88
	30	19.3/0.72	23.0/0.78	22.9/0.76	24.8/0.81	21.6/0.75	29.7/0.80
	40	15.4/0.65	17.0/0.67	18.5/0.69	19.7/0.72	17.6/0.64	23.6/0.76
	50	12.5/0.60	15.4/0.63	16.4/0.66	17.1/0.68	15.1/0.62	21.2/0.72
	10	20.7/0.54	21.3/0.58	22.4/0.61	24.1/0.65	21.1/0.59	25.5/0.71
	20	18.8/0.52	20.6/0.55	21.6/0.57	23.2/0.62	20.4/0.57	24.9/0.69
	30	16.9/0.49	19.6/0.53	20.5/0.54	22.6/0.58	18.6/0.51	23.7/0.66
	40	15.1/0.47	17.7/0.51	20.1/0.53	21.4/0.55	18.0/0.51	22.1/0.62
	50	12.0/0.43	16.2/0.48	18.4/0.50	19.9/0.52	17.1/0.49	21.5/0.57
	10	24.4/0.66	26.2/0.71	28.2/0.74	29.3/0.76	27.9/0.73	32.1/0.80
	20	23.1/0.64	25.5/0.68	27.8/0.71	28.8/0.74	25.2/0.69	31.3/0.77
	30	21.7/0.61	24.4/0.66	26.5/0.69	27.1/0.72	26.5/0.67	30.6/0.74
	40	18.3/0.59	21.6/0.62	23.3/0.65	26.4/0.70	22.3/0.64	29.2/0.73
	50	17.6/0.55	19.8/0.61	22.1/0.63	24.6/0.67	20.3/0.62	28.2/0.71
	10	21.8/0.64	23.7/0.68	26.2/0.74	26.3/0.74	23.5/0.69	29.1/0.79
	20	20.3/0.61	22.2/0.67	25.1/0.71	25.3/0.72	21.8/0.66	28.3/0.77
	30	19.5/0.58	21.3/0.65	24.4/0.68	25.0/0.69	20.7/0.67	27.0/0.75
	40	18.2/0.56	20.6/0.64	23.8/0.66	24.1/0.67	19.3/0.62	26.5/0.72
	50	17.3/0.55	19.7/0.61	22.6/0.63	23.2/0.65	18.8/0.59	25.7/0.71

Table 4 Continue.....






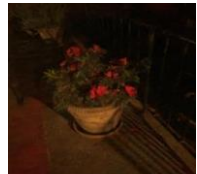
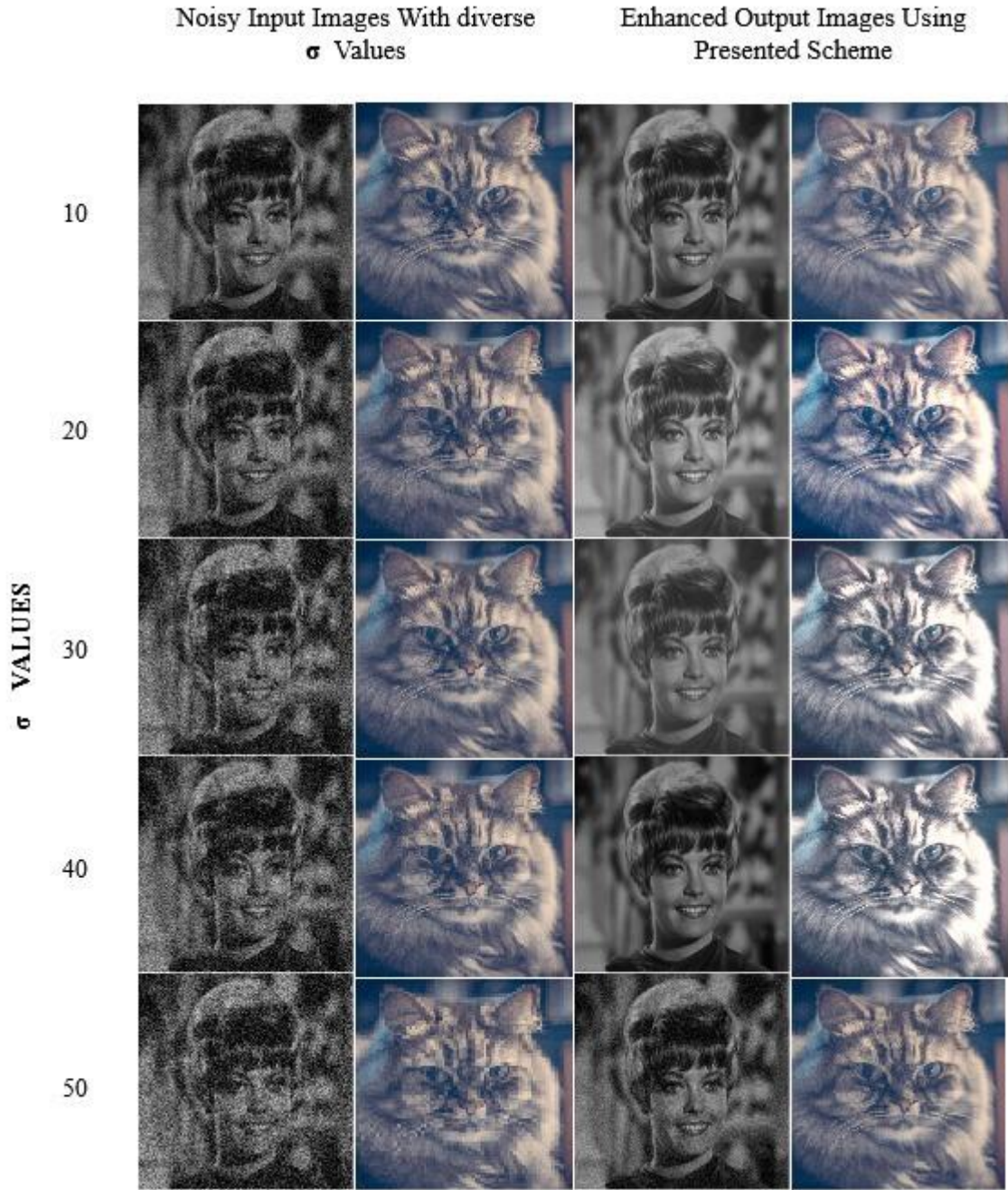
Test Sample Images	$\sigma$ Rate	Ying <i>et al.</i> 2017	Lore <i>et al.</i> 2017	Atoum <i>et al.</i> 2020	Zhang, <i>et al.</i> 2020	DnCNN	Proposed Method
	10	28.6/0.77	29.9/0.82	29.4/0.81	31.4/0.84	29.2/0.80	33.4/0.88
	20	27.1/0.75	28.0/0.77	28.6/0.79	30.2/0.81	28.1/0.78	32.5/0.85
	30	26.9/0.75	27.3/0.76	27.9/0.77	28.8/0.79	27.4/0.76	30.8/0.82
	40	25.3/0.71	26.1/0.73	27.0/0.74	28.1/0.76	26.6/0.73	29.2/0.79
	50	23.7/0.68	24.8/0.70	25.5/0.72	27.3/0.74	24.4/0.69	28.6/0.77
	10	26.4/0.75	27.6/0.77	27.8/0.79	28.4/0.82	27.1/0.78	32.2/0.83
	20	26.1/0.72	27.5/0.75	27.2/0.76	27.8/0.79	26.7/0.74	31.3/0.81
	30	25.5/0.70	26.7/0.73	27.0/0.74	27.4/0.77	26.5/0.73	30.8/0.80
	40	25.2/0.69	26.0/0.71	26.3/0.72	26.9/0.74	25.9/0.70	30.4/0.80
	50	23.4/0.63	24.2/0.69	25.2/0.70	25.3/0.71	24.1/0.68	28.5/0.78
	10	27.3/0.84	27.8/0.87	29.3/0.88	30.2/0.89	27.7/0.84	32.4/0.91
	20	27.0/0.81	27.2/0.85	28.7/0.86	29.3/0.88	27.5/0.82	31.7/0.89
	30	25.3/0.76	26.3/0.80	26.9/0.80	27.8/0.81	25.6/0.77	29.9/0.86
	40	23.4/0.72	24.7/0.74	25.1/0.75	26.7/0.77	24.6/0.72	28.6/0.85
	50	22.5/0.69	24.2/0.72	24.4/0.72	25.1/0.75	24.1/0.71	28.2/0.84
	10	22.5/0.64	23.3/0.68	23.4/0.67	24.1/0.69	23.1/0.66	26.5/0.73
	20	20.8/0.61	22.6/0.67	22.6/0.56	23.2/0.68	22.4/0.65	25.9/0.71
	30	20.1/0.59	21.6/0.63	21.5/0.62	22.6/0.65	21.2/0.63	24.7/0.69
	40	19.1/0.57	21.2/0.62	21.1/0.61	21.4/0.63	20.2/0.60	23.8/0.68
	50	18.6/0.56	19.2/0.59	19.0/0.58	20.2/0.60	19.1/0.58	22.7/0.66
	10	27.4/0.76	28.2/0.81	28.4/0.84	29.3/0.86	27.9/0.79	33.1/0.91
	20	27.1/0.74	27.7/0.78	28.0/0.81	28.8/0.84	27.2/0.76	32.3/0.87
	30	26.7/0.71	27.4/0.74	27.6/0.77	28.1/0.79	27.0/0.72	30.6/0.85
	40	23.9/0.67	26.6/0.70	26.7/0.70	27.1/0.73	25.1/0.69	29.2/0.80
	50	22.6/0.63	24.8/0.66	25.1/0.67	25.6/0.69	23.3/0.65	28.5/0.76
	10	21.4/0.68	23.6/0.71	24.2/0.73	25.3/0.75	23.5/0.71	28.7/0.80
	20	20.9/0.65	22.7/0.68	23.1/0.70	24.4/0.72	22.4/0.68	28.3/0.78
	30	20.5/0.63	21.3/0.66	22.4/0.67	23.6/0.69	21.2/0.66	27.8/0.76
	40	18.6/0.58	20.6/0.64	21.8/0.63	22.1/0.65	19.3/0.63	27.0/0.73
	50	17.5/0.54	19.7/0.60	21.6/0.62	21.2/0.62	18.1/0.59	26.2/0.71

Table 4 displays the results. Enhancing a noisy picture and displaying its PSNR and SSIM were accomplished using Ying's method, DnCNN, attention-based networks, and a proposed

hybrid DWT+SA+DnCNN. DWT and attention-based DSD-trained suggested technologies work best across the board in image quality. Our DWT+SA+DnCNN outperforms baseline DnCNN as well. Figure 6 demonstrates that for the tested levels of noise exposure, the restored images produced by the hybrid DnCNN suffer no discernible quality loss.



**Figure 6.** Restoration results of proposed methodology under various  $\sigma$  values  
 Different denoising methods were extensively tested and compared. Table 4 shows that



compared to traditional methods, the DnCNN algorithm and attention-based networks perform better. Because the proposed model is a direct adaptation of DnCNN and SA-based networks, we compare our response to theirs. Here's a rundown of how our hybrid DnCNN and standard DnCNN are similar with respect to their parameters: By decreasing the number of layers to 10, we were able to reduce the number of trainable parameters from 350 to 12% (with masked weights). It is important to note that only 88% of the reported parameters contribute to the output of the hybrid DnCNN. The DnCNN training took about 130 minutes, whereas the DWT-SA-DnCNN training took about 280 minutes. The proposed energy-based DnCNN network dramatically shortens the average denoising time (14 seconds) by 60%.

For hybrid Gaussian ( $\sigma = 30$ ) and impulsive noise (40%) conditions, Table 5 shows the outcomes of both specific and general methods used to get rid of noise. After applying denoising to the test images, it displays the average PSNR, MSE, and SSIM statistics. Raising the total number of training iterations did not greatly enhance the outcomes, whether it was for specific noise level restoration (35 iterations) or non-particular noise level denoising (50 iterations). For each noise scenario in the testing set, the system executed for 25 iterations, and then the average measurements of assessment were tabulated.

**Table 5.** Analysis of the mean squared error (MSE), peak signal-to-noise ratio (PSNR), and structural similarity index (SSIM) for the fusion of impulse and Gaussian noises on the SET14, SET5 and SID dataset.

Image Enhancement Strategies	Assessment Metrics for the Methodologies		
	<i>MSE</i>	<i>PSNR</i>	<i>SSIM</i>
CLAHE	87.2539	21.3586	0.7716
DHE	86.6583	23.5410	0.7801
Fu's Method	84.8127	26.4378	0.8181
Ying's Method	80.9320	27.4213	0.8435
VGG-16	79.6642	28.0194	0.8896
DnCNN	76.1254	29.3267	0.9089
LLNet	73.2901	30.8761	0.9118
Gladnet	72.9654	30.8723	0.9278
Attention-based network	72.8521	31.3365	0.9414
Suggested Scheme	<b>70.0452</b>	<b>33.2546</b>	<b>0.9621</b>

The table 5 provides an assessment of different image-enhancing approaches using three commonly used evaluation metrics: mean squared error (MSE), peak signal-to-noise ratio (PSNR), and structural similarity index (SSIM). The Contrast Limited Adaptive Histogram Equalization (CLAHE) approach, exhibits a mean squared error (MSE) value of 87.2539, a peak signal-to-noise ratio (PSNR) of 21.3586, and a structural similarity index (SSIM) of 0.7716. The Dynamic Histogram Equalization (DHE) method achieves an MSE (mean squared error) of 86.6583, a PSNR (peak signal-to-noise ratio) of 23.5410, and an SSIM (structural similarity index) of 0.7801. Fu's Method, Ying's Method, and deep learning-based models such as VGG-16, DnCNN, LLNet, and Gladnet demonstrate gradual enhancements in performance. The attention-based network demonstrates superior performance compared to several other techniques, as evidenced by its mean squared error (MSE) of 72.8521, peak signal-to-noise ratio (PSNR) of 31.3365, and structural similarity index (SSIM) of 0.9414. The suggested scheme demonstrates satisfactory equilibrium with a mean squared error (MSE) of 70.0452, a peak signal-to-noise ratio (PSNR) of 33.2546, and a structural similarity index (SSIM) of 0.9621, indicating its effectiveness in improving image quality. Overall, the measures together offer a thorough assessment, uncovering the advantages presented approach in terms of enhancing image quality.

**Table 6.** Average running time (Seconds) assessment of the presented scheme

Method	HE	DHE	Ying's Method	Attention-based network	DnCNN	Suggested Scheme Without Attention Module	Suggested Scheme With Attention Module
Time (s)	589.38	475.53	173.70	92.38	130.24	98.54	14.33

Table 6 displays the correlation between the running time (in seconds) and various filter sizes and input images used to analyze a  $256 \times 256$  image. The results are obtained by calculating the mean value from 20 separate trials conducted on various photos. In terms of training duration, a local basis denoiser requires approximately 10.5 hours, while a nonlocal basis denoiser needs around 13 hours, assuming that the filter sizes are both set to  $2 \times 2$ . The complete training duration for DWT-SA-DnCNN is around 1.5 days.

## 5. CONCLUSION

The idea and approaches can be applied to detect and remove many forms of unidentified noise in the domain of image restoration. This comprehensive method has the potential to be extremely effective in a variety of complex signal and image processing procedures that frequently suffer from noise. This study domain has the potential for further development to encompass clinical image processing, biometrics technology, and telecommunications, amongst other applications. This paper proposes a method for enhancing images using a discrete wavelet transform and an attention-based denoising convolutional neural network. The hybrid wavelet transforms with a self-attention-based dense-sparse-dense retraining strategy were effectively utilized in the DnCNN, leading to the development of an extremely effective hybrid denoising structure with significantly reduced layers and characteristics. The primary goal is to utilize the proposed approach to develop a denoising model capable of identifying noise, determining its impact, and enhancing the filtering system's pattern to minimize noise. The proposed method has the ability to effectively eliminate several types of noise, either individually or in combination, even when the noise levels are at their highest. Furthermore, it consistently produces results that closely resemble the clean, noise-free image, which is a distinctive characteristic of this method. Results show our technique best performs on the SID and real-time image databases, producing images of greater quality with reduced noise and chromatic distortions. We aim to develop a more efficient focus module to reduce computing costs and enhance system applicability in future research.

## REFERENCES

- [1].Abdullah-Al-Wadud M., Kabir M H., Dewan M A A., & Chae O. (2007). A dynamic histogram equalization for image contrast enhancement. *IEEE Transactions on Consumer Electronics*, 53(2), 593-600.
- [2].Ai, S., & Kwon, J. (2020). Extreme low-light image enhancement for surveillance cameras using attention U-Net. *Sensors*, 20(2), 495.
- [3].Alawode B O., Masood M., Ballal T., & Al-Naffouri T. (2021). Dense-Sparse Deep CNN Training for Image Denoising. *arXiv preprint arXiv:2107.04857*
- [4].Alisha P B, & Gnana Sheela K. (2016). Image Denoising Techniques-An Overview, *IOSR Journal of Electronics and Communication Engineering*, Vol. 11, pp.: 78-84, 2016. (C-3).
- [5].Al-Najjar Y A., & Soong D C. (2012). Comparison of image quality assessment: PSNR, HVS, SSIM, UIQI. *Int. J. Sci. Eng. Res*, 3(8), pp. 1-5.



- [6].Asha S., & Sreenivasulu G. (2018). Satellite Image Enhancement Using Contrast Limited Adaptive Histogram Equalization. *Int. J. Sci. Res. Sci. Eng. Technol*, 4, 1070-1075.
- [7].Atoum, Y., Ye, M., Ren, L., Tai, Y., & Liu, X. (2020). Color-wise attention network for low-light image enhancement. In *Proceedings of the IEEE/CVF Conference on Computer Vision and Pattern Recognition Workshops* (pp. 506-507).
- [8].Banik, P. P., Saha, R., & Kim, K. D. (2018, January). Contrast enhancement of low-light image using histogram equalization and illumination adjustment. In *2018 international conference on electronics, information, and Communication (ICEIC)* (pp. 1-4). IEEE.
- [9].Bassiou, N., & Kotropoulos, C. (2007). Color image histogram equalization by absolute discounting back-off. *Computer Vision and Image Understanding*, 107(1-2), 108-122.
- [10].Chen, C., Chen, Q., Xu, J., & Koltun, V. (2018). Learning to see in the dark. In *Proceedings of the IEEE conference on computer vision and pattern recognition* (pp. 3291-3300).
- [11].Dominici D., Zollini S., Alicandro M., Della Torre F., Buscema P M., & Baiocchi, V. (2019). High resolution satellite images for instantaneous shoreline extraction using new enhancement algorithms. *Geosciences*, 9(3), 123. <https://doi.org/10.3390/geosciences9030123>
- [12].Fan L., Zhang, F., Fan, H., & Zhang, C. (2019). Brief review of image denoising techniques. *Visual computing for industry, biomedicine, and art*, 2(1), 7. <https://doi.org/10.1186/s42492-019-0016-7>
- [13].Fu X., Liao Y., Zeng D., Huang Y., Zhang X P., & Ding X. (2015). A probabilistic method for image enhancement with simultaneous illumination and reflectance estimation. *IEEE Transactions on Image Processing*, 24(12), 4965-4977. <https://doi.org/10.1109/TIP.2015.2474701>.
- [14].Fu X., Wang J., Zeng D., Huang Y., & Ding X. (2015). Remote sensing image enhancement using regularized-histogram equalization and DCT. *IEEE Geoscience and Remote Sensing Letters*, 12(11), 2301-2305.
- [15].Gonzalez R C., Woods R E., & Masters B R. (2009). *Digital Image Processing*, Third Edition. *J. Biomed. Opt.* 2009, 14, 029901.
- [16].Guo X., Li Y., & Ling H. (2016). LIME: Low-light image enhancement via illumination map estimation. *IEEE Transactions on image processing*, 26(2), 982-993.
- [17].Han B G., Yang H S., & Moon Y S. (2018). Locally adaptive contrast enhancement using convolutional neural network. In *2018 IEEE International Conference on Consumer Electronics (ICCE)* (pp. 1-2). IEEE. <http://doi.org/10.1109/ICCE.2018.8326096>
- [18].Han S., Pool J., Narang S., Mao H., Gong E., Tang S., & Dally W J. (2016). DSD: Dense-sparse-dense training for deep neural networks. *arXiv preprint arXiv:1607.04381*.
- [19].He K., Zhang X., Ren S., & Sun J. (2016). Deep residual learning for image recognition. In *Proceedings of the IEEE conference on computer vision and pattern recognition*. pp. 770-778. doi: 10.1109/CVPR.2016.90.

- [20].Hu L., Qin M., Zhang F., Du Z., & Liu R. (2021). RSCNN: A CNN-Based Method to Enhance Low-Light Remote-Sensing Images. *Remote Sensing*, 13(1), 62. <https://doi.org/10.3390/rs13010062>.
- [21].Ibrahim H., & Kong N S P. (2007). Brightness preserving dynamic histogram equalization for image contrast enhancement. *IEEE Transactions on Consumer Electronics*, 53(4), 1752-1758.
- [22].Ioffe S., & Szegedy C. (2015). Batch normalization: Accelerating deep network training by reducing internal covariate shift. In *International conference on machine learning*. PMLR-37, pp. 448-456.
- [23].Jain V., Murray J F., Roth F., Turaga S., Zhigulin V., Briggman K L., & Seung H S. (2007, October). Supervised learning of image restoration with convolutional networks. In *2007 IEEE 11th International Conference on Computer Vision*. pp. 1-8.
- [24].Jobson, D. J., Rahman, Z. U., & Woodell, G. A. (1997). A multiscale retinex for bridging the gap between color images and the human observation of scenes. *IEEE Transactions on Image processing*, 6(7), 965-976.
- [25].Karthikeyan, V., Raja, E., & Pradeep, D. (2023). Energy based denoising convolutional neural network for image enhancement. *The Imaging Science Journal*, 1-16.
- [26].Kaur R., Juneja M., & Mandal A K. (2018). A comprehensive review of denoising techniques for abdominal CT images. *Multimedia Tools and Applications*, 77(17), pp: 22735-22770. doi:<http://dx.doi.org/10.1007/s11042-017-5500-5>
- [27].Kim J., Lee J K., & Lee K M. (2016). Accurate image super-resolution using very deep convolutional networks. In *Proceedings of the IEEE conference on computer vision and pattern recognition*. pp. 1646-1654.
- [28].Land, E. H. (1977). The retinex theory of color vision. *Scientific american*, 237(6), 108-129.
- [29].Lee D., Kim K H., Kang H E., Wang S H., Park S Y., & Kim J H. (2015). Learning speed improvement using multi-gpus on dnn-based acoustic model training in korean intelligent personal assistant. In *Natural Language Dialog Systems and Intelligent Assistants*. pp. 263-271. Springer, Cham.
- [30].Lee E., Kim S., Kang W., Seo D., & Paik J. (2012). Contrast enhancement using dominant brightness level analysis and adaptive intensity transformation for remote sensing images. *IEEE Geoscience and remote sensing letters*, 10(1), 62-66.
- [31].Li C., Guo J., Porikli F., & Pang Y. (2018). LightenNet: A convolutional neural network for weakly illuminated image enhancement. *Pattern recognition letters*, 104, 15-22.
- [32].Li L., Wang R., Wang W., & Gao W. (2015). A low-light image enhancement method for both denoising and contrast enlarging. In *2015 IEEE International Conference on Image Processing (ICIP)* (pp. 3730-3734). IEEE.
- [33].Liu C., Cheng I., Zhang Y., & Basu A. (2017). Enhancement of low visibility aerial images using histogram truncation and an explicit Retinex representation for balancing contrast and color consistency. *ISPRS Journal of Photogrammetry and Remote Sensing*. 128. 16-26. 10.1016/j.isprsjprs.2017.02.016.

- [34].Liu Z., Yan W Q., & Yang M L. (2018). Image denoising based on a CNN model. 2018 4th International Conference on Control, Automation and Robotics (ICCAR), IEEE. pp: 389-393.
- [35].Lore K G., Akintayo A., & Sarkar S. (2017). LLNet: A deep autoencoder approach to natural low-light image enhancement. Pattern Recognition, 61, 650-662. <https://doi.org/10.1016/j.patcog.2016.06.008>
- [36].Ma X., Wang D., Liu D., & Yang J. (2020). DWT and CNN based multi-class motor imagery electroencephalographic signal recognition. Journal of neural engineering, 17(1), 016073.
- [37].Pisano E D., Zong S., Hemminger B M., DeLuca M., Johnston R E., Muller K., & Pizer, S M (1998). Contrast limited adaptive histogram equalization image processing to improve the detection of simulated spiculations in dense mammograms. Journal of Digital imaging, 11(4), 193.
- [38].Portilla J., Strela V., Wainwright M J., & Simoncelli E P. (2003). Image denoising using scale mixtures of Gaussians in the wavelet domain. IEEE Transactions on Image processing, 12(11), 1338-1351.
- [39].Rahman Z U., Jobson D J., & Woodell . A. (1996, September). Multi-scale retinex for color image enhancement. In Proceedings of 3rd IEEE International Conference on Image Processing, Vol. 3, pp. 1003-1006.
- [40].Shelhamer E., Long J., & T. Darrell T. (2017) "Fully Convolutional Networks for Semantic Segmentation," in IEEE Transactions on Pattern Analysis and Machine Intelligence, 39(4), pp. 640-651. [http:// 10.1109/TPAMI.2016.2572683](http://10.1109/TPAMI.2016.2572683)
- [41].Shen, L., Yue, Z., Feng, F., Chen, Q., Liu, S., & Ma, J. (2017). Msr-net: Low-light image enhancement using deep convolutional network. arXiv preprint [arXiv:1711.02488](https://arxiv.org/abs/1711.02488).
- [42].Singh P., & Shree R. (2020). Impact of Method Noise on SAR Image Despeckling. International Journal of Information Technology and Web Engineering (IJITWE), 15(1), 52-63.
- [43].Tao L., Zhu C., Song J., Lu T., Jia H., & Xie X. (2017, September). Low-light image enhancement using CNN and bright channel prior. In 2017 IEEE International Conference on Image Processing (ICIP) (pp. 3215-3219). IEEE.
- [44].Toshev A., & Szegedy C. (2014). Deeppose: Human pose estimation via deep neural networks. In Proceedings of the IEEE conference on computer vision and pattern recognition (pp. 1653-1660).
- [45].Wang, X., Bai, X., Li, G., Sun, L., Ye, H., & Tong, T. (2023). Noise Attenuation for CSEM Data via Deep Residual Denoising Convolutional Neural Network and Shift-Invariant Sparse Coding. Remote Sensing, 15(18), 4456.
- [46].Wang, W., Wei, C., Yang, W., & Liu, J. (2018, May). Gladnet: Low-light enhancement network with global awareness. In 2018 13th IEEE international conference on automatic face & gesture recognition (FG 2018) (pp. 751-755). IEEE.
- [47].Wang Z., & Bovik A C. (2002). A universal image quality index. IEEE signal processing letters, 9(3), pp. 81-84.

- [48].Wang Z., Bovik A C., Sheikh H R., & Simoncelli E P. (2004). Image quality assessment: from error visibility to structural similarity. IEEE transactions on image processing, 13(4), 600-612.
- [49].Xie J., Xu L., & Chen E. (2012). Image denoising and inpainting with deep neural networks. In Advances in neural information processing systems. pp. 341-349.
- [50].Ying Z., Li G., Ren Y., Wang R., & Wang W. (2017). A New Low-Light Image Enhancement Algorithm Using Camera Response Model. 2017 IEEE International Conference on Computer Vision Workshops (ICCVW), 2017, pp. 3015-3022, doi: 10.1109/ICCVW.2017.356.
- [51].Zhang, C., Yan, Q., Zhu, Y., Li, X., Sun, J., & Zhang, Y. (2020, July). Attention-based network for low-light image enhancement. In 2020 IEEE international conference on multimedia and expo (ICME) (pp. 1-6). IEEE.
- [52].Zhang K., Zuo W., Chen Y., Meng D., & Zhang L. (2017). Beyond a gaussian denoiser: Residual learning of deep cnn for image denoising. IEEE transactions on image processing, 26(7), pp. 3142-3155.
- [53].Zollini S., Alicandro M., Cuevas-González M., Baiocchi V., Dominici D., & Buscema, P M. (2020). Shoreline extraction based on an active connection matrix (ACM) image enhancement strategy. Journal of Marine Science and Engineering, 8(1), 9. <https://doi.org/10.3390/jmse8010009>